Sensors and Materials, Vol. 35, No. 7 (2023) 2413–2432
MYU Tokyo

S & M 3332

Reducing Surge Voltage and Ringing Effect of DC Voltage Converter by Transient Suppressor

Wei Chien,[1,2,3] Chien-Ching Chiu,[4*] Po-Hsiang Chen,[4]
Jie-Xian Zhuo,[1] Jiang Hao,[5] and Cheng-Lun Tsai[4]

[1]Department of School of Electric and Information Engineering,
Beibu Gulf University, Qinzhou 535011, P.R. China
[2]Guangxi Key Laboratory of Ocean Engineering Equipment and Technology, Qinzhou 535011, P.R. China
[3]Key Laboratory of Beibu Gulf Offshore Engineering Equipment and Technology, Beibu Gulf University,
Education Department of Guangxi Zhuang Autonomous Region, Qinzhou 535011, P.R. China
[4]Department of Electrical and Computer Engineering, Tamkang University, New Taipei City 25137, Taiwan
[5]School of Engineering, San Francisco State University, San Francisco, CA 94117-1080, USA

(Received April 7, 2023; accepted June 26, 2023)

Keywords: buck converter, snubber, switching power

Sensors are common electronic products in daily life, and the stability of their power supply is important. In electromagnetic interference (EMI), electromagnetic signals interfere with sensors, which in severe cases may reduce the accuracy of the sensor measurement. We use snubbers to suppress the electromagnetic interference so that the sensors can operate under stable conditions. As the energy source of electrical operations, a power supply is essential in every electronic system. Direct current (DC) provides the main internal operating power in commonly used electronic products. In this paper, the DC voltage converter (switching buck) is described, which can lead to a more stable DC voltage to increase the operation stability, lifetime, and reliability of electronics. The results of this study can be used to design electronic systems that are more stable and reliable and to extend the life of systems with a DC power supply. This study also leverages the positive effects of a snubber on circuits while having little effect on the overall circuit, even with the addition of electric circuits. By using different resistances and capacitances to conduct experiments on actual products and comparing the results, a buffer circuit was optimized for different needs to remove its negative effects. This approach enables designers to optimize snubber circuits for different circuit requirements. Furthermore, detailed experiments and analyses of snubber circuits provide an understanding of the importance of power supplies in electrical circuits and establish a basis for future improvements and developments. Moreover, the near-field radiation, EMI, and eye pattern are investigated for electronic countermeasures. The analysis provides not only qualitative discussion but also quantitative research. These results are helpful and useful for circuit designers.

*Corresponding author: e-mail: chiu@ee.tku.edu.tw
https://doi.org/10.18494/SAM4447

ISSN 0914-4935

1. Introduction

In the era of rapid development of science and technology, in order to bring convenience to people, sensors are widely used daily. However, every electronic product needs a power supply, the essential component that serves as the source of its operation. The main operating power of these systems is from DC. However, a computer runs with AC, which is supplied from a wall socket to a low-voltage DC power supply in the computer. In addition, as each component in the computer needs a stable and continuous power supply, the power supply must be equipped with a voltage regulator/stabilizer to provide accurate and stable voltage to ensure the normal operation of the components. A "power supply rail" or "voltage rail" generally refers to the various voltages provided by the power supply.[1–17]

The power supply of the first generation of microcomputers and home personal computers was linear and composed of a heavy step-down transformer combined with a rectifier, a filter element, and a voltage regulator. Modern computers use a switching-mode power supply after the main power supply is directly rectified and filtered. An isolated DC–DC conversion device is composed of a high-frequency switching device such as a bipolar junction transistor or MOSFET and a ferrite core high-frequency step-down transformer. The device reduces and stabilizes DC power. The output of the filter device is electrical energy for the computer. A switching-mode power supply is much lighter, cheaper, and more efficient than a linear power supply.[2,3,10,12,17]

At present, pulse width modulation-type switching power converters and non-isolated DC–DC converters with switching inductance are predominantly used because of their low cost and mature technology. There are three basic electrical structures: buck type, boost type, and boost and buck type. This medium- and low-power converter (DC–DC converter) uses MOSFETs, which are the most commonly used switching elements. During the operation of the circuit, the voltage between the drain and the source is close to an ideal square wave. However, the stored current of the inductor on the line is cut off instantaneously, which generates a high-voltage surge and high-frequency oscillation with stray capacitance. Because of the impact of semiconductor switching elements in the circuit, a circuit designer uses a buffer circuit to protect or increase its rated value. The commonly used buffer circuit of the switching power converter is a passive (turn-off) type that suppresses the voltage drop and the accompanying oscillation when the switching element is turned off.[4,5,9,11,13]

With the improvement of technology, portable electronic products are becoming increasingly advanced. Therefore, all portable electronic products, such as mobile phones, tablets, laptops, and digital cameras, are developing into devices that are lighter and thinner and have more functions while taking up limited space. However, as more functions are added, the number of circuits in each product increases. Therefore, it is necessary to optimize the efficiency and life of the circuit and electronic components.[2,9–17]

DC–DC converters are now widely used in numerous electronic systems. The development of portable electronic products for personal use requires that they run faster every 3 years. In the 1970s, the power supply industry began to adopt MOSFETs that used switching regulators. The high-power conversion efficiency or flexibility of MOSFETs was optimal for many machines and became the mainstream of power supplies.[6] Hegarty showed that synchronous buck

converters generally switch under 3 MHz but generate broadband noise and electromagnetic interference (EMI) up to 1 GHz.[7] He presented a novel technique of spread-spectrum frequency modulation that disperses the spectral energy of the switching signal; and a substantial improvement was obtained. The eye diagram of the signal was affected by the technique.[7] Liu *et al.* proposed a snubber design method specialized for solid-state circuit breaker overvoltage suppression at bus fault interruption, because the traditional method suited for the converter switch snubber cannot be directly applied to a solid-state circuit breaker. However, the method can only be used after the parameters are determined.[8] Zaman *et al.* proposed a gate driver with an RC snubber that eliminates crosstalk by maintaining any spurious gate spike below the gate threshold voltage, since at high switching frequency, the crosstalk phenomenon occurs when the gate voltage spike introduced by high dv/dt and voltage ringing forces the false turn-on of silicon carbide MOSFETs, which causes a crow-bar current there.[9] Furthermore, the proposed driver circuit does not require a dedicated negative voltage source, and voltage feedback and is realized using low-cost components. However, the signal quality for a high-definition multimedia interface (HDMI) was slightly reduced.[9] Cheng *et al.* searched for an advantageous switching pattern that reduces the total switching loss of two power devices in an inverter circuit and constrains the surge voltage simultaneously. However, this optimization method has a large computational burden.[10] Yano *et al.* presented a method for optimally designing resistor–inductor (RL) and resistor–capacitor (RC) snubber circuits to reduce the electromagnetic interference caused by parasitic inductor–capacitor (LC) resonance.[11] The effects of the snubbers were reproduced by a simulation program with an integrated circuit to validate the method from the perspective of resonance damping, overshoot, and power loss. However, an analytical method for optimally designing the RC snubbers has not been developed.[11]

A lossless snubber cell for a soft-switched bidirectional buck-boost converter has been proposed by Joo and Han.[12] The proposed snubber cell does not have any auxiliary switch; therefore, no complex auxiliary circuits or driving algorithms for the auxiliary switch are required. However, the validity for applying the proposed snubber cell to the bidirectional inverter has not been investigated.[12] Mohammadi *et al.* presented a new lossless passive snubber for the bidirectional buck-boost converter.[13] Excellent efficiency is acquired over a wide load range by using a simple auxiliary circuit and the conventional control methods. The experimental results of a 500 W–100 kHz prototype for both the boost and buck modes in full load and 20% of full load are given to confirm the theoretical analysis. However, the method requires complex frequency control to reduce the circulating current from the auxiliary inductor capacitor resonant circuit, especially under light load conditions.[13] Power system designers have been endeavoring to find a power conversion design that is more flexible, more reliable, and better performing under various power frequency and load conditions. Yau and Hung proposed an active dissipative snubber to suppress the resonance in the discontinuous conduction mode.[16] The digital controller activates the dissipative snubber only when the EMI noise is occurring, then, the snubber is disabled after the noise is decayed or disappears. Digital logic makes the passive snubber smart, which can selectively absorb the EMI noise. Since the proposed snubber is not connected to the main circuit all the time, it can provide lower power

loss, but still has better EMI emissions and maintains conversion efficiency.[16] However, not all snubbers can provide a soft-switching condition at turn-on and turn-off transients.[17]

However, as a result of the switching element of the power converter, the line parasitic capacitance and inductance generate a voltage surge with a high-frequency oscillating voltage waveform, causing damage to the elements and generating electromagnetic interference and circuit instability. An appropriate buffer circuit suppresses high-frequency oscillating waves and solves the above problems. However, the circuit also increases costs and reduces efficiency. Besides, the designer usually focuses on the advantage and ignores the disadvantage. Moreover, most studies do not deal with the HDMI signal. Most transient voltage suppressors often solve the electromagnetic interference problem without meeting the overall required transmission rate. In this paper, we focus on HDMI signals, which have rarely been discussed in previous research. The innovation is that our proposed method can use snubbers to suppress the electromagnetic interference and meet the electromagnetic compatibility (EMC) specification even after the printed circuit board (PCB) has been laid out. In addition, it can meet the eye diagram specification standard at a high transfer rate. In this paper, we aim to provide the design principles of the cut-off passive buffer circuit (snubber) and discuss mainly the fine-tuning of the added electronic countermeasures for HDMI circuits in case the user EMI requirements could not be met and when the PCB wiring could no longer be changed. Physical measurements to verify its effect of suppressing high-frequency oscillating waves and analysis of the impact on the overall circuit can help product designers optimize the buffer circuit for different needs to remove their negative impact. Moreover, the near-field radiation, EMI, and eye pattern are investigated for the electronic countermeasures. The analysis results provide not only qualitative discussion but also quantitative research. These results are helpful and useful for the circuit designer. In Sect. 2, the system model and improvement method are described. Numerical results and discussion are presented in Sect. 3. In Sect. 4, the conclusion for reducing the surge voltage and ringing effect of the DC voltage converter is given.

2. System Model and Improvement Method

A snubber is a device in the switching power supply system. When the power component is switched, the overlapping of voltage and current causes considerable power loss, especially because of the stray inductance in the circuit. A considerable surge in voltage and current occurs during switching. When the operation of the components exceeds a safe limit, the power component is damaged as a result. Power semiconductor components such as bipolar transistors, field-effect transistors, thermistors, and insulated gate bipolar transistors operate normally without damaging the voltage or current.

For example, for the field-effect transistor, the horizontal coordinate of the safe working limit is the drain-source voltage (V_{DS}), and the vertical coordinate is the drain-source current (I_D). The range of safe working limits is defined by a drawn curve. This boundary curve combines the following working limits of the device: maximum voltage, maximum current, and dissipation power. These limits also include the temperature of the butt joint, internal thermal resistance, the current-carrying ability of a die bonding wire, and secondary collapse.

In addition to defining the safe zone according to continuous working conditions, a safe working limit under the pulse wave is established for instantaneous working conditions (for example, 1 or 10 mS).[18]

The snubber circuit is designed to protect power components.[19,20] The major effect is the elimination of the surge voltage when the switch is transformed. The traditional power converter uses the power switch to control the conduction of energy. To reduce the volume and weight of the converter for higher power density, it is necessary to increase the switching frequency of the converter. However, when the converter operates and causes high-frequency switching, the inherent loss increases, while the efficiency of the converter decreases. To solve the problem of the many losses caused by a converter at high frequencies, we used a soft-switching technology to reduce the loss. As a result, we improved the performance of the boost converter, which has been demonstrated through simulations. The soft-switching technology uses an active buffer circuit to reduce the loss of the circuit switch. The loss is caused by the reverse recovery characteristics of the diode, which is also improved by the active buffer circuit and the performance of the boost converter. The components of the active buffer circuit comprise two diodes, a capacitor, an inductor, and an auxiliary switch. A passive snubber circuit is mainly divided into two types: (1) turn-on snubber and (2) turn-off snubber.

As shown in Fig. 1, the conduction type mainly functions to delay the switching time and the climbing of the slope to provide buffering during switching.[6] The cut-off snubber circuit used in this paper was the RC cut-off type, which is the most popular. As shown in Fig. 2, the operating principle is as follows: R is the resistor and C is the capacitor.[8]

When a MOSFET is turned off, the voltage V_{ds} starts to rise, and the capacitor C is charged through the resistor R. When the MOSFET is turned on, the energy in C is discharged through R and the MOSFET. The snubber circuit absorbs the power that is consumed by the MOSFET to protect the circuit. Figure 3 shows the effect of adding the snubber circuit.[20] In the cut-off circuit of the RC snubber, the time constants for charging and discharging are determined by R and C, so it is difficult to select the R and C values in the design. Generally, the R value is about 1 to 5 Ω, whereas the C value is 1000 pF to 10 nF.

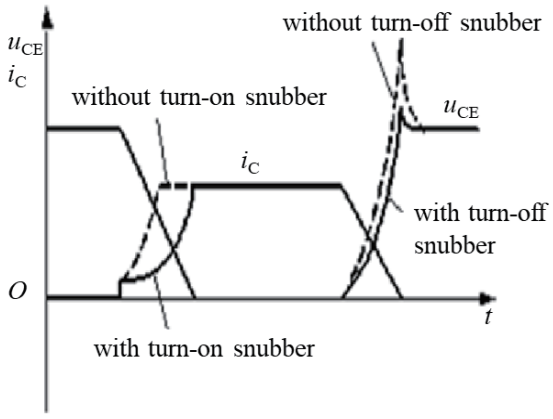

Fig. 1. Turn-on snubber and turn-off snubber.

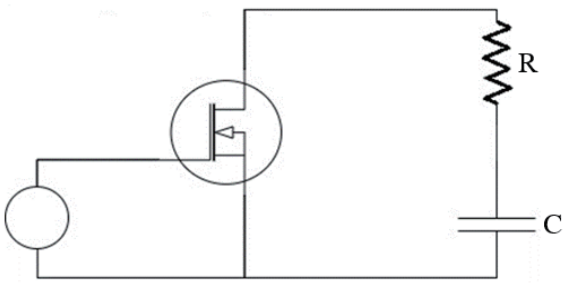

Fig. 2. Snubber circuit.

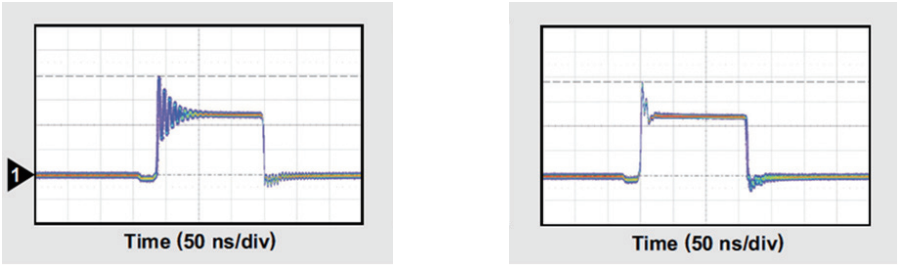

(a) (b)

Fig. 3. (Color online) Performance of the snubber. (a) Ringing with hight-side gate resistor (5 V/div) and (b) ringing with snubber (5 V/div).

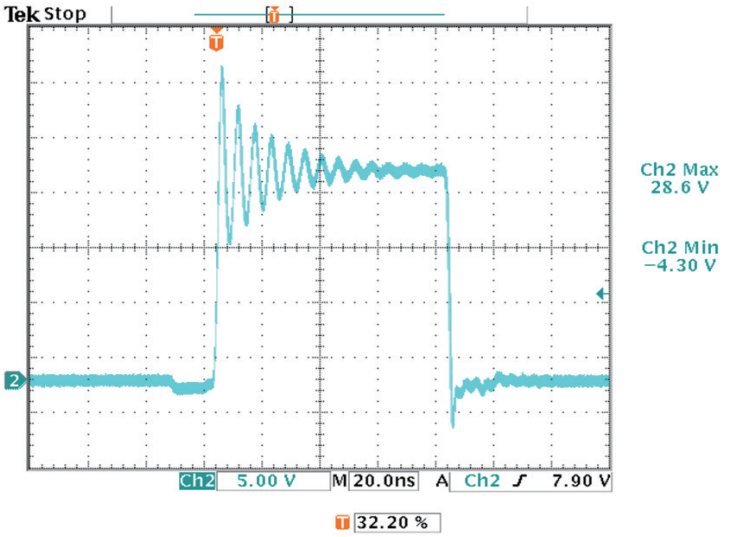

Fig. 4. (Color online) Ringing wave.

Ringing occurs at the moment that the power switch is shifted. Ringing in electronics refers to unwanted oscillations in voltage or current, potentially because of the parasitic capacitance and inductance in the circuit caused by the pulse wave (not a component added to the design, but a side effect due to the material or placement in the circuit). The ringing generates parasitic capacitance and inductance in the circuit to resonate at its characteristic frequency. Ringing also appears in the square wave. As shown in Fig. 4, the sudden pulse wave causes the parasitic capacitance and inductance in the circuit to become the system signal. However, it is not the oscillation that is expected when the circuit is designed.

On the other hand, the frequency of switching ringing is high and far exceeds the switching frequency that accompanies a high-voltage surge. This results in conduction and radiated EMI problems. The main radiation source in the buck converter is the input switching circuit of the converter with the disadvantage of an EMI. The EMI problem is reflected in the experimental results in Fig. 5. The ringing frequency falls between 150 and 250 MHz. Moreover, it interferes with the normal operation of the signal circuit of the switching power supply or other nearby functional circuits. Therefore, suppressing the ringing of the switch is an important part of the

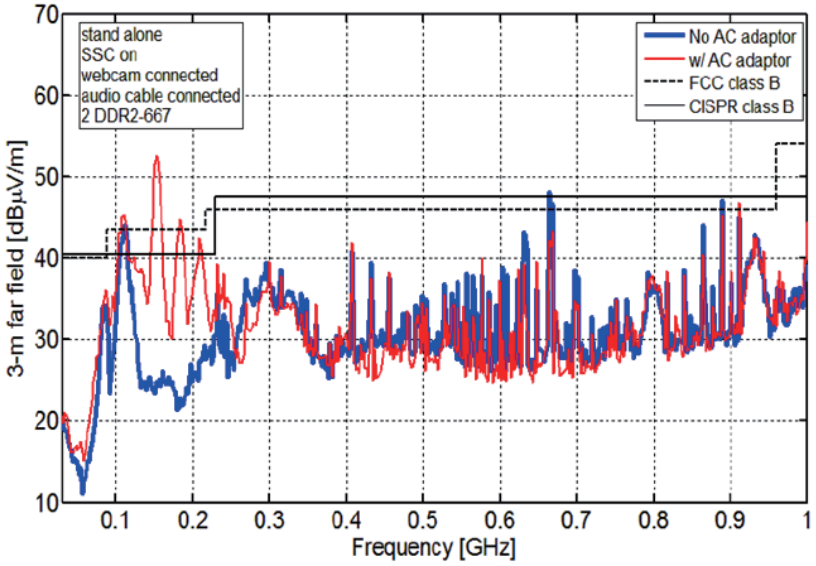

Fig. 5. (Color online) EMI problem in experimental results.

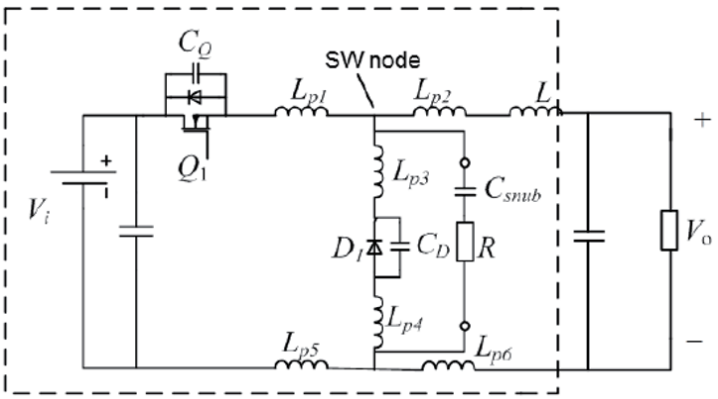

Fig. 6. Buck circuit containing the main parasitic inductance and capacitance.

design of the switching power supply. The snubber is the most commonly used method, especially when the above measures do not achieve the best results because of limitations of objective factors. The snubber changes the ringing frequency, and its capacitance effect reduces the dV/dt of the switching node, thereby effectively suppressing EMI.

Figure 6 shows a buck circuit that contains the main parasitic inductance and capacitance. The RC snubber is placed between the switch node and the GND node. This circuit mainly suppresses the ringing when the top switch is turned on, and the ringing is the source of most MOSFET overvoltage and EMI problems.

First, because the switching process is completed quickly (from several to several tens of nanoseconds), the current of the inductor L is almost unchanged during this process, so L and L_{p2} (including the series L_{p6}) are not involved in the ringing. Second, after the ringing causes the

amplitude to exceed V_i, the channel of the high-side MOSFET is fully opened. C_Q is short-circuited and is not involved in the ringing. The circuit can be regarded as equivalent to the LC resonant circuit in Fig. 6. The new L_R and C_R are the compound values of all parasitic inductances and capacitances involved in ringing, which are L_{p1}, L_{p5}, L_{p3}, and L_{p4}. Generally, the snubber's C_{snub} value is above 1 nF, and the impedance at the ringing frequency F_R (after adding the snubber) is very small. R is normally above a few ohms, so the left of Fig. 7 is further approximated to the right side of Fig. 7.

According to the circuit in Fig. 7, we derived Eq. (1).

$$V_i = \frac{L_r C_r d^2 u_c}{dt^2} + \frac{L_r du_c}{R_{snub} dt^2} + u_c \tag{1}$$

Therefore, to dampen the ringing in the circuit,

$$R \geq \frac{\sqrt{\left(\frac{L_R}{C_R}\right)}}{2}. \tag{2}$$

Figure 8 is a comparison chart of simulations using Allegro/OrCAD after including different resistance values. The other conditions of the simulation are $L_{p1} = L_{p5} = 10$ nH; $L_{p3} = L_{p4} = 2$ nH; $C_{snub} = 10$ nF; and CD = 200 pF. When $R = \frac{1}{2}\sqrt{(L_R / C_R)}$, the voltage amplitude is the lowest.

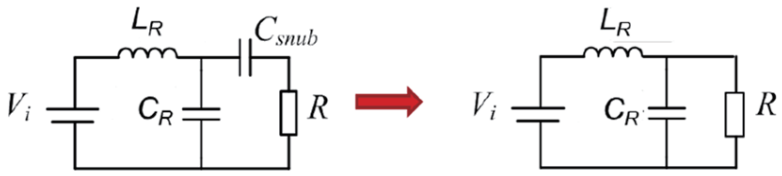

Fig. 7. (Color online) Equivalent circuit with high side ringing.

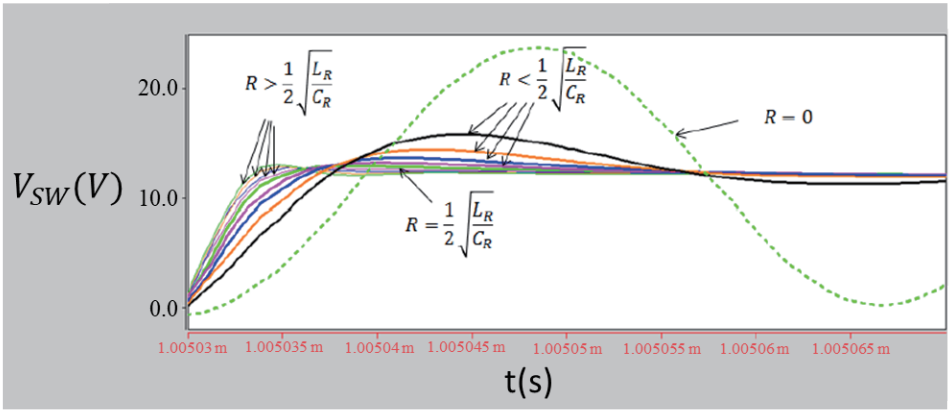

Fig. 8. (Color online) Comparison chart after introducing different resistance values.

It is also important that the larger the value of C_{snub}, the greater the loss of the buck circuit and the worse the efficiency. The loss includes two aspects. First, the loss on the snubber resistor is proportional to the capacitance value of the capacitor. The previous equations can be used to derive the following equation.

$$P_{Snub} = \frac{1}{2} \times C_{Snub} \times V_{(SWpeak)^2} \times F_{sw} \tag{3}$$

Here, $V_{(SWpeak)^2}$ is the peak ringing frequency and F_{SW} is the switching frequency. Figure 9 shows the ringing effect for different capacitances and the same resistance.

Figure 10 shows the corresponding relationship between the driving voltage when the high-side MOSFET turns on and the current–voltage on the MOSFET.[21] The equation is the MOSFET switching loss (including turn-on and turn-off losses; it is assumed that the turn-on

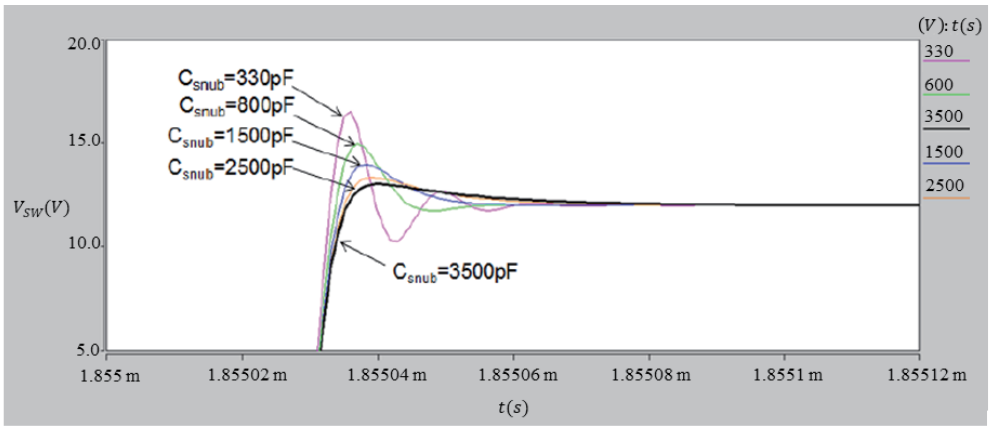

Fig. 9. (Color online) Effect of the same resistance with ringing.

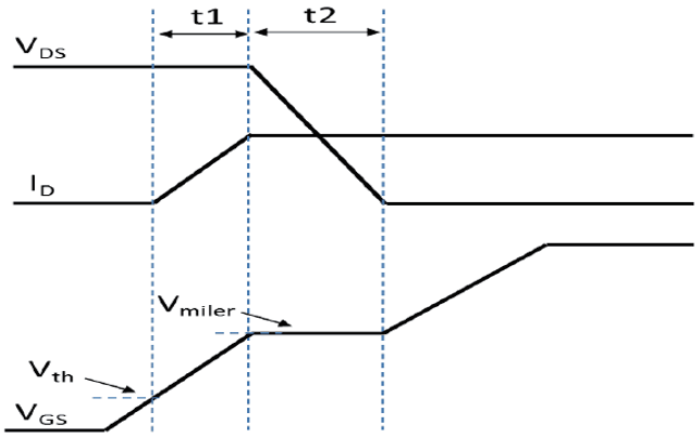

Fig. 10. Corresponding relationship wave in opening.

and turn-off times are the same) because t_2 increases with the increase in C_{snub}, and the switching loss also increases accordingly. It is clear that a smaller capacitor is better from the perspective of a smaller loss.

$$P_{SW} = (t_1 + t_2) \times V_{sw} \times I_{sw} \times F_{sw} \tag{4}$$

3. Results and Discussion

The use of transient voltage suppressors in a buck conversion circuit experiment is discussed in this paper. The experimental platform was a ZenBook UX310UV produced by ASUS. We measured the efficiency, energy consumption, and temperature of the buck conversion circuit separately. The basic architecture of the RT8248A buck converter used in this study is shown in Fig. 11.

The test environment of the RT8248A buck circuit was set up as follows.

(1) A DC power supply provides the 19 V DC input power required by the motherboard. The maximum peak supply current of the power supply needs to be at least 2 A.
(2) The input port of the test board is connected to the output of the DC power supply to obtain the power of the start-board IC and each group of DC–DC converters.
(3) Through the function of the DC electronic load (smart electronic load), the load phenomenon of the terminal equipment is simulated.
(4) An oscilloscope is used to intercept the MOSFET waveform and obtain its original waveform, as shown in Fig. 12.

The ringing frequency obtained from Fig. 12 is F_n = 80.6 MHz and C_{OSS} = 900 pF at V_{in} = 6 V. Thus, we obtained $R_{snub} = \dfrac{1}{2\pi \mathcal{F}_n C_{oss}}$ = 2.19 Ω. Then, the appropriate capacitance value C_{snub} was selected.

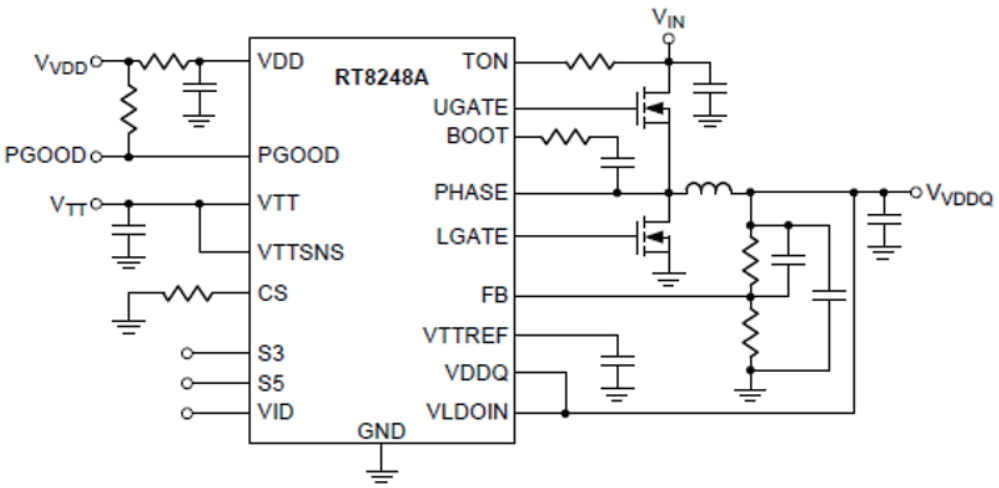

Fig. 11. RT8248A architecture.

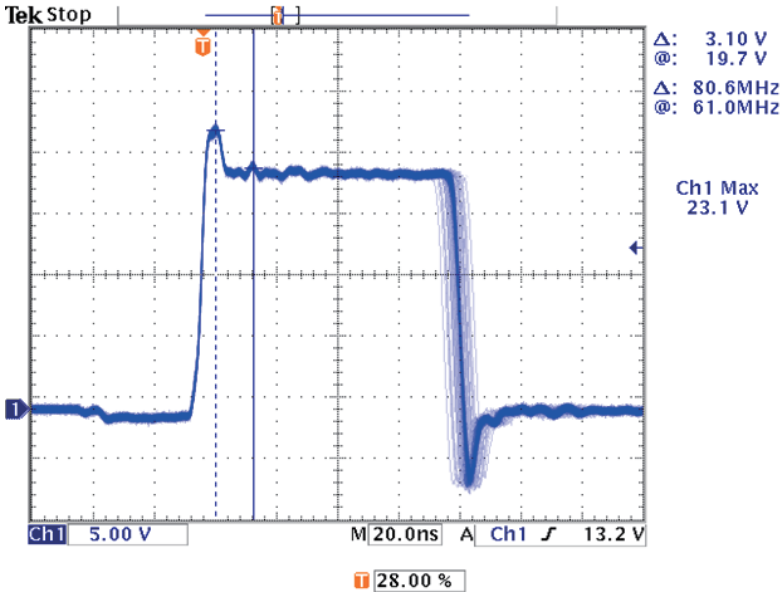

Fig. 12. (Color online) Measurement of a ringing wave.

As mentioned earlier, the choice of capacitance is a compromise between amplitude suppression and loss control. With the following equation as a starting point, further adjustments are needed according to the loss and amplitude suppression effect. After increasing the capacitance to suppress the amplitude and reducing the capacitance to improve efficiency,[21] we obtained C_{snub} = 3608 pF.

Here, the efficiency is defined as the ratio of the converted output power to the input power. This is the same as in the step-down conversion circuit. In the following equation, I_{cc} is the output current, and I_{out} is the current consumption of the IC itself. However, since this current is extremely small, it is ignored when the load current is large. When the input and output currents are the same, it is calculated as the output voltage divided by the input voltage.

$$Efficiency\ formula: efficiency = \frac{output\ power}{input\ power} \times 100\% \tag{5}$$

Here, $input\ power = V_{in} \times I_{in}$ and $output\ power = V_{out} \times I_{out}$.

3.1 Efficiency experiment

The setup for the experimental measurement of efficiency of the RT8248A buck circuit is shown in Fig. 13. A DC power supply provides board-side power so that the buck IC RT8248A can be powered up. In addition to the input source of its buck converter circuit, the test circuit has an independent power supply to avoid interference with other power supplies in the motherboard and effects on the efficiency calculation.

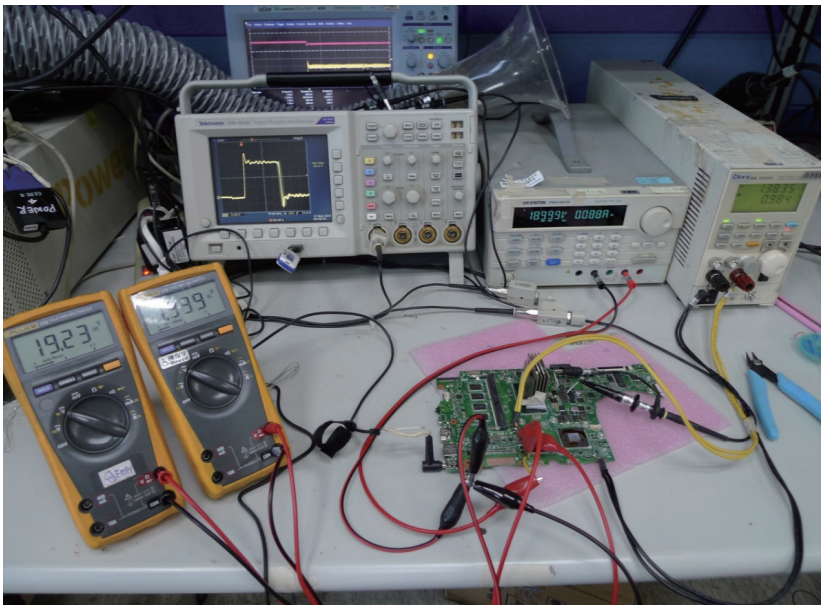

Fig. 13. (Color online) Setup used to measure the RT8248A step-down circuit efficiency.

A three-electric meter measured the input voltage V_{in} and output voltage V_{out}. A current meter measured the input current I_{in} and the output current I_{out} using the load machine to simulate its output. The output current was 5 A, which was simulated into ten different loads. For each section, 0.5 A was output by the load machine, and the data were measured and recorded.

As shown in Fig. 14, adding resistance and capacitance had different effects on the efficiency of the original circuit. Increasing capacitance had an especially strong influence. It was observed that changing the capacitance had a marked effect on efficiency: the difference was about 1 to 2%. Furthermore, it was observed that changing the resistance had a substantial effect on efficiency, with a difference of about 0.2 to 0.5%.

The importance of capacitance is expressed by the following equation.

$$P_{Snub} = \frac{1}{2} \times C_{Snub} \times V_{(SWpeak)^2} \times F_{sw} \tag{6}$$

As the development of the power supply and the pursuit of saving power require a higher conversion efficiency, a product with low efficiency loses its competitiveness.

3.2 Energy consumption experiment

The analysis in Fig. 15 shows that regardless of which resistance value is used, the energy consumption significantly increases with the change in the capacitance value. The

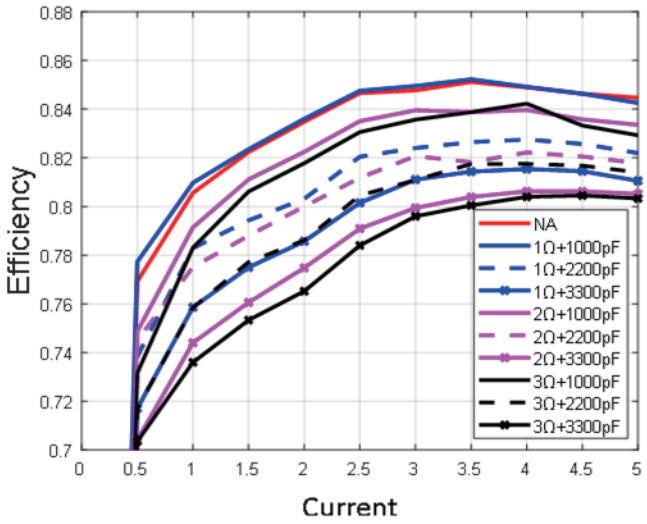

Fig. 14. (Color online) Experimental efficiency.

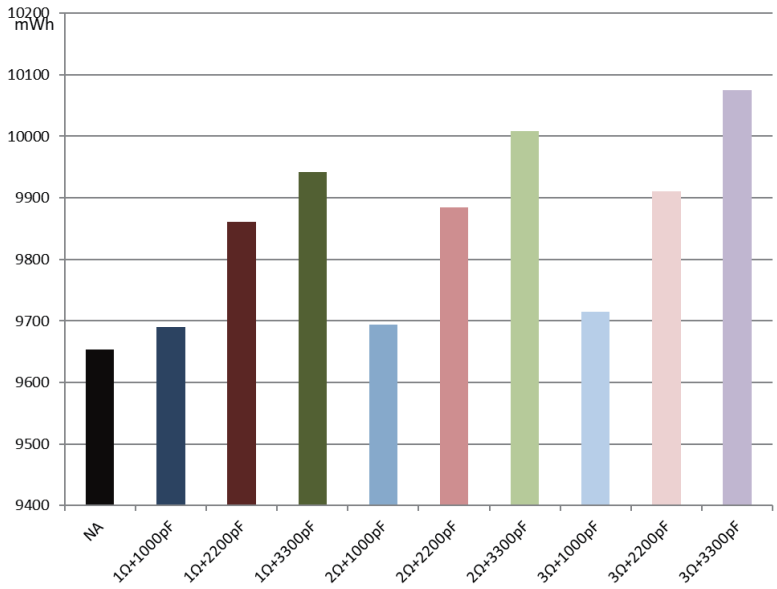

Fig. 15. (Color online) Comparison chart of energy consumption for fixed resistance.

higher the capacitance value, the greater the increase in energy consumption. The analysis in Fig. 16 reveals that regardless of which capacitor value is used, the energy consumption significantly increases with a change in the resistance value. The higher the resistance value, the greater the increase in energy consumption.

In the experiment, the addition of R_{snub} and C_{snub} to the switching power converter significantly increased its energy consumption. The impact on the circuit itself depended on the R_{snub} and C_{snub} values. The maximum difference between the experiments was around 4.4%. The increase in the capacitance and the resistance affected the energy consumption and increased the capacitance.

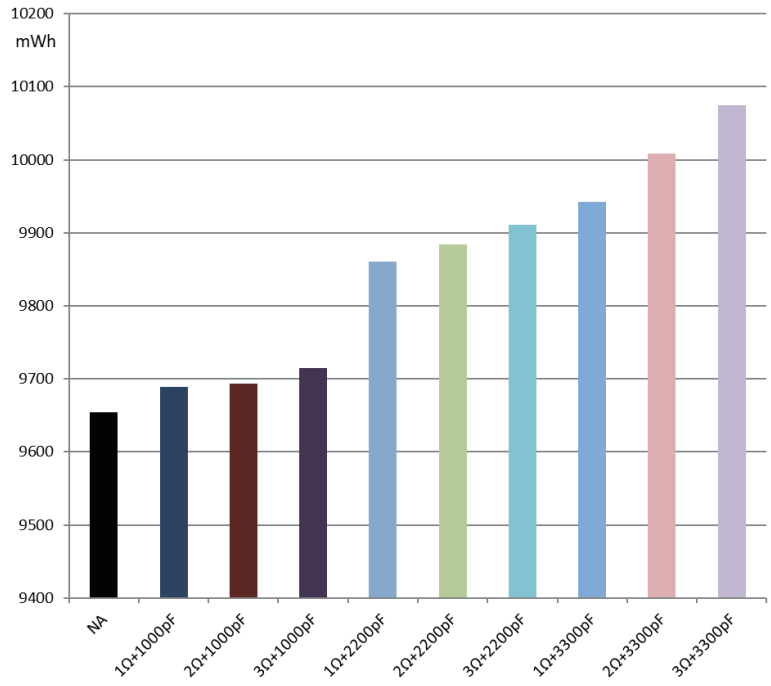

Fig. 16. (Color online) Comparison chart of energy consumption for a fixed capacitor.

In the analysis of energy consumption, we adopted the same test method as in many power supply safety certifications in various countries around the world. The addition of resistance and capacitance had a maximum effect of 5% on the circuit for only one of dozens of power supplies. Many products today require long-term use, which is directly reflected in battery life.

3.2 Temperature experiment

Figure 17 shows the temperature values of the main components after experimental measurement using a temperature recorder, Mobile Corder. The main components of the step-down switching power converter (HI-SIDE, LO-SIDE, CHOKE, IC, snubber) were recorded by the temperature recorder. The temperature increased slightly with R_{snub} and C_{snub}. The increase in R_{snub} and C_{snub} did not significantly increase the temperature and had a minimal effect on the circuit. Observations of the other main components in the circuit indicated that the temperature of the switch MOS in the circuit dropped because the snubber circuit participated in sharing the surge energy when the switch was shifted.

3.3 Snubber waveform measurement experiment

We experimentally measured the resistance and capacitance values in the experiment to determine whether it was actually effective in suppressing the surge voltage and ringing. By comparing the difference in the results with and without a snubber in Figs. 18

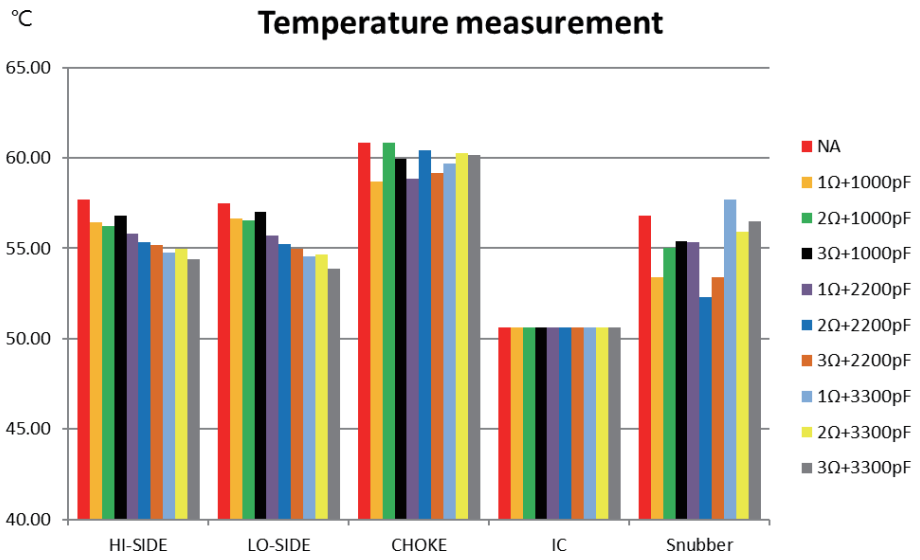

Fig. 17. (Color online) Experimental temperature summary chart.

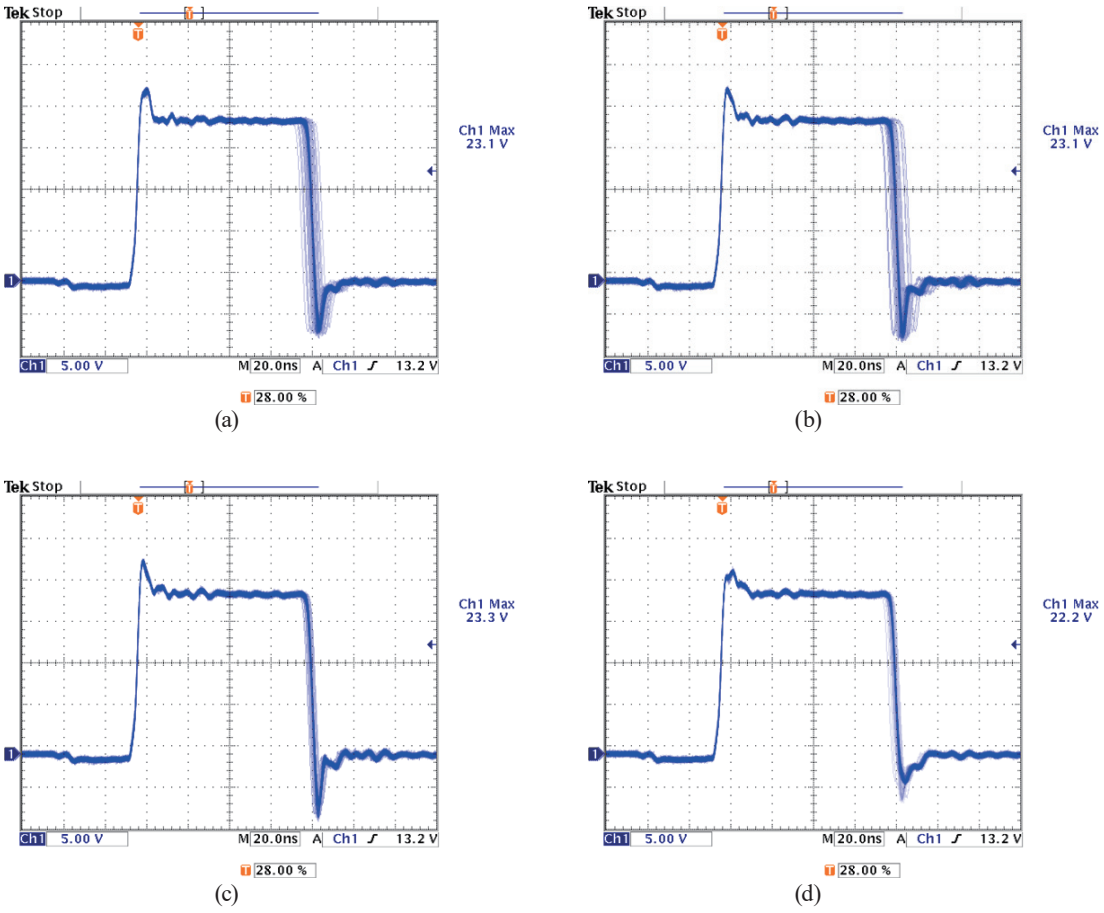

Fig. 18. (Color online) Measurement of the snubber waveform. (a) 1 Ω + 1000 pF, (b) 2 Ω + 1000 pF, (c) 3 Ω + 1000 pF, and (d) 1 Ω + 2200 pF.

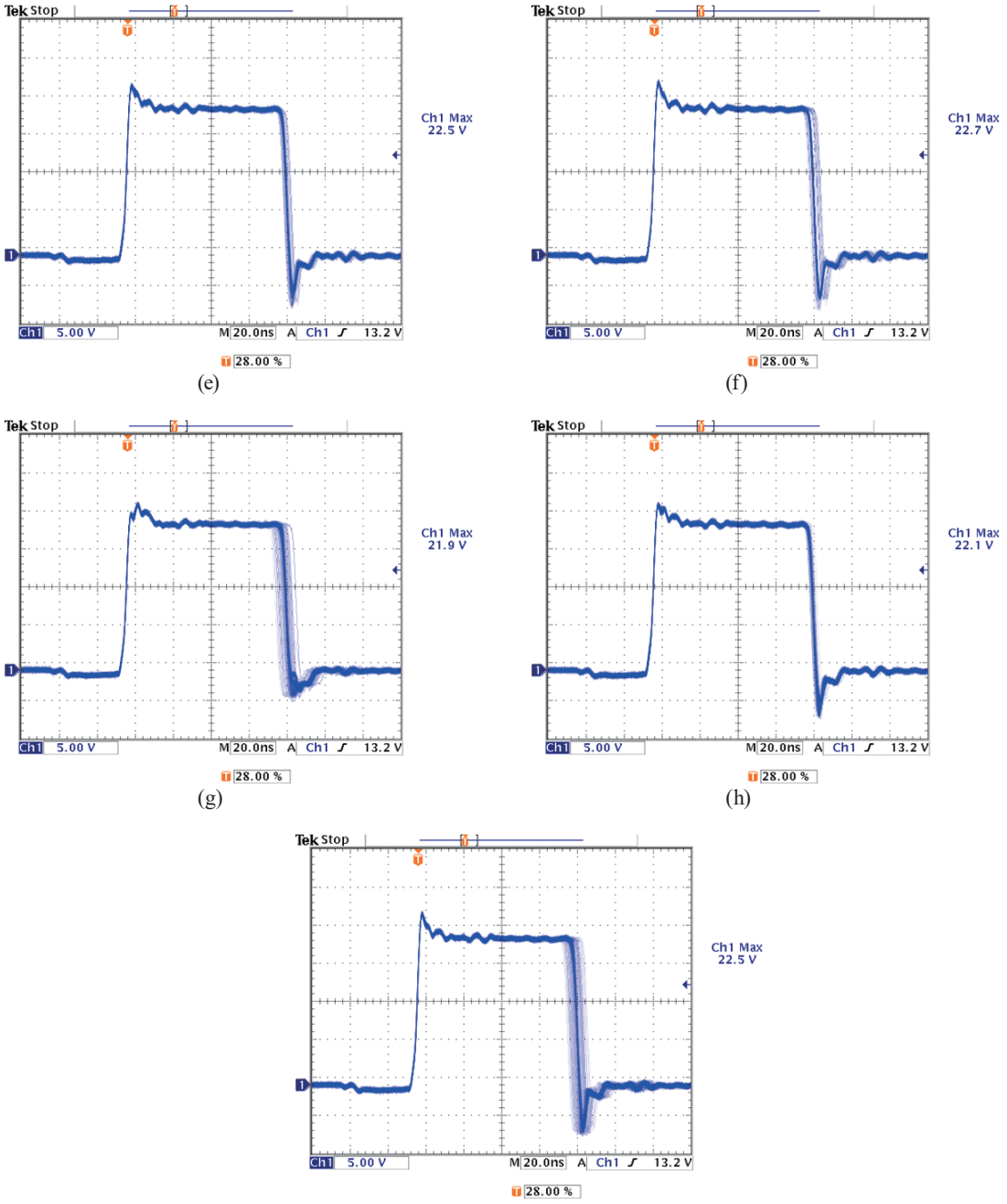

Fig. 18. (Continued) (Color online) Measurement of the snubber waveform. (e) 2 Ω + 2200 pF, (f) 3 Ω + 2200 pF, (g) 1 Ω + 3300 pF, (h) 2 Ω + 3300 pF, and (i) 3 Ω + 3300 pF.

and 19, it was observed that the suppression effect was significant for conditions of R_{snub} = 2.19 Ω (the closest value was 2 Ω) and C_{snub} = 3608 pF (the closest value was 3300 pF).

This experiment showed that the best waveform suppression effect was close to the calculated value, but in practice, the value was always fixed because of cost. Thus, designers must be attentive to calculation results; otherwise, the expected suppression effect is not achieved, and the overall efficiency and energy consumption effects are lost.

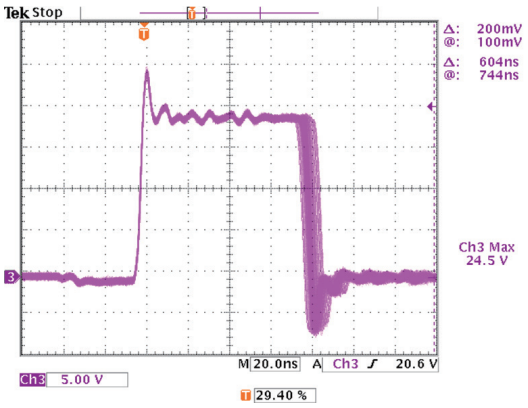

Fig. 19. (Color online) Results without using the snubber waveform.

Table 1
Summary of all experimental data.

Snubber Solution	EFF (%)	W	Thermal	Spike
NA	85.41	9653.64	57.51	24.5
1 Ω + 1000 pF	85.23	9689.4	56.63	23.3
2 Ω + 1000 pF	83.88	9693.72	56.55	23.1
3 Ω + 1000 pF	83.88	9714.84	57.00	23.3
1 Ω + 2200 pF	82.64	9860.52	55.72	22.2
2 Ω + 2200 pF	81.82	9884.52	55.22	22.5
3 Ω + 2200 pF	81.74	9910.8	54.98	22.7
1 Ω + 3300 pF	81.43	9942.12	54.56	21.9
2 Ω + 3300 pF	80.39	10008.36	54.66	22.1
3 Ω + 3300 pF	80.05	10074.48	53.90	22.5

All the experimental data are summarized in Table 1. The results show that the addition of a snubber had a positive effect on the original circuit, but there are still non-negligible negative effects. The voltage surge and the possible EMI effects caused by the ringing problem were solved. However, the snubber yielded poor conversion efficiency and increased energy consumption. Therefore, an ideal combination of a suitable voltage suppression circuit and the product requirements needs to be specific to the characteristics of the product.

4. Conclusions

In this paper, a DC voltage converter (switching buck) was added to the transient voltage suppressor to buffer and suppress its surge voltage and ringing, and the results were measured and analyzed. Circuit designers are required to test the positive effect of the transient voltage suppressor on the circuit and the effect of adding a circuit on the overall circuit. The best output demanded for high-performance games does not require energy or power saving. However, business computers need extremely high power-saving abilities and long product life for long-term durability and cost reduction. Therefore, a single design method does not meet all of today's

needs. Designing a circuit according to product characteristics is the focus of all future 3C power supply designs.

In this study, we added electronic countermeasures for HDMI circuits in case the user EMI requirements could not be met and when the PCB wiring could no longer be changed, and we compared the near-field radiation distribution, EMI, and eye pattern before and after taking the electronic countermeasures. In case the PCB layout could not be adjusted again, in this study, we adopted the common mode choke and parallel resistance for treatment. Moreover, we measured the far-field and near-field variations. The results show that the common mode choke has the ability to inhibit the common mode signal of differential signals, but according to the measurement results, the improvement of EMI is limited, and although the parallel connection of differential signals with high resistance has significant effects on EMI, it has greater effects on the quality of differential signals. Thus, through practical studies, it is found that a parallel resistance of 330 ohm has little effect on the signal quality but has some effect on EMI attenuation; therefore, it accords more to economic profit in terms of costs. The analysis provides not only qualitative discussion but also quantitative research and can also provide an effective reference for the circuit designer. In addition, our proposed snubber can bring stable power to sensors and electronic products.

Acknowledgments

This research is supported by the Guangxi Higher Vocational Education Reform Project (GXGZJG2020A001).

References

1 J. C. Salmon: Proc. 1995 IEEE Appli. Power Electron. Conf. and Exp. (1995 IEEE) 473–479.
2 T. Dai, J. Qin, G. Ge, C. Zhou, L. He, J. Zhai, and J. Li: IEEE Access **8** (2020) 61421. https://doi.org/10.1109/ACCESS.2020.2983090
3 B. Zhao, Q. Song, W. Liu, and Y. Sun: IEEE Trans. Power Electron. **8** (2014) 4091. https://doi.org/10.1109/TPEL.2013.2289913
4 H. Dong, X. Xie, and L. Zhang: IEEE Trans. Power Electron. **35** (2020) 4457. https://doi.org/10.1109/TPEL.2019.2944492
5 T. J. Liang, K. H. Chen, and J. F. Chen: IEEE Trans. Power Electron. **33** (2018) 3604. https://doi.org/10.1109/TPEL.2017.2709811
6 A. Elasser and D. A. Torrey: IEEE Trans. Power Electron. **11** (1996) 710. https://doi.org/10.1109/63.535403
7 T. Hegarty: Analog Appli. J. Texas Instruments, Inc. AAJ 3Q (2016).
8 F. Liu, W. Liu, X. Zha, H. Yang, and K. Feng: IEEE Trans. Power Electron. **32** (2017) 3007. https://doi.org/10.1109/TPEL.2016.2574751
9 H. Zaman, X. Wu, X. Zheng, S. Khan, and H. Ali: Energies **11** (2018) 3111. https://doi.org/10.3390/en11113111
10 Y. S. Cheng, T. Mannen, K. Wada, K. Miyazaki, M. Takamiya, and T. Sakurai: IEEE Trans. Ind. Appl. **55** (2019) 5023. https://doi.org/10.1109/TIA.2019.2927462
11 Y. Yano, N. Kawata, K. Iokibe, and Y. Toyota: IEEE Trans. Electron. Compa. **61** (2019) 1217. https://doi.org/10.1109/TEMC.2018.2841424
12 H. I. Joo and S. K. Han: IEEE Access **8** (2020) 165708. https://doi.org/10.1109/ACCESS.2020.3022397
13 M. R. Mohammadi, H. Farzanehfard, and E. Adib: IEEE Trans. Ind. Electron. **67** (2020) 8363. https://doi.org/10.1109/TIE.2019.2947850
14 J. Bačmaga and A. Barić: IEEE Trans. Electron. Compa. **63** (2021) 2124. https://doi.org/10.1109/TEMC.2021.3069546

15 M. A. Alarcón-Carbajal, J. E. Carvajal-Rubio, J. D. Sánchez-Torres, D. E. Castro-Palazuelos, and G. J. Rubio-Astorga: Energies **15** (2022) 5288. https://doi.org/10.3390/en15145288
16 Y.-T. Yau and T.-L. Hung: IEEE Access **10** (2022) 108145. https://doi.org/10.1109/ACCESS.2022.3204872
17 M. R. Mohammadi: IEEE Trans. Ind. Electron. **67** (2020) 1396. https://doi.org/10.1109/TIE.2019.2901642
18 T. Williams: The Circuit Designer's Companion (Elsevier, Oxford, 2004) 2nd ed., pp. 129–130.
19 A. Elasser and D. A. Torrey: IEEE Trans. Power Electron. **11** (1996) 710. https://doi.org/10.1109/63.535403
20 S. Lee, H. Choe, and B. Kang: IEEE Trans. Power Electron. **33** (2018) 2026. https://doi.org/10.1109/TPEL.2017.2698211
21 K. M. Smith and K. M. Smedley: IEEE Trans. Power Electron. **16** (2001) 336. https://doi.org/10.1109/63.923765

About the Authors

Wei Chien was born in Taipei, Taiwan, Republic of China, on April 21, 1974. He received his B.S.C.E. degree from Ta Tung University, Taipei, in 1997 and his M.S.E.E. degree from Tamkang University, Taipei, in 1999. From 1999 to 2001, he served in the ROC Army Force and was an assistant in the Department of Electrical Engineering. From 2007 to 2014, he was an assistant professor in the Department of Electronic Engineering, De Lin Institute of Technology. From 2014 to 2017, he was a professor in the Department of Computer Engineering, Ningde Normal University. Since 2017, he has been a professor in the Department of Electric and Information Engineering, Beibu Gulf University. His research area is deep learning for inverse scattering. (air180@seed.net.tw)

Chien-Ching Chiu received his B.S.C.E. degree from National Chiao Tung University, Hsinchu, Taiwan, in 1985 and his M.S.E.E. and Ph.D. degrees from National Taiwan University, Taipei, in 1987 and 1991, respectively. From 1987 to 1989, he was a communication officer with the ROC Army Force. In 1992 he joined the Department of Electrical Engineering, Tamkang University, where he is now a professor. From 1998 to 1999, he was a visiting scholar at Massachusetts Institute of Technology, Cambridge, and the University of Illinois at Urbana-Champaign, USA. He was a visiting professor with the University of Wollongong, Australia, in 2006, with the University of London, United Kingdom, in 2011, and with University Tunku Abdul Rahman, Malaysia, from 2019 to 2020. His current research interests include inverse problems, deep learning for microwave imaging, indoor wireless communications, and simultaneous wireless information and power transfer systems. He has published more than 150 journal papers on inverse scattering problems, communication systems, and optimization algorithms. (chiu@ee.tku.edu.tw)

Po-Hsiang Chen received his B.S. degree from HungKuo Delin University of Technology, Tucheng, Taiwan, in 2017 and M.S. degree from Tamkang University, Tamsui, Taiwan, in 2020. Since 2021, he has been working toward his Ph.D. degree at the Department of Electrical and Computer Engineering, Tamkang University. His research areas are inverse scattering and deep learning. (810440031@gms.tku.edu.tw).

Jie-Xian Zhuo was born in Liuzhou, Guangxi, China on December 18, 1967, and graduated from the College of Physical Education and Health of Guangxi Normal University in June 1990. Professor Zhuo worked in Liuzhou Teachers College in Guangxi (now Guangxi Science and Technology Normal University) from July 1990 to August 2012. She was an on-the-job postgraduate student of Curriculum and Instruction at the College of Physical Education and Health of Guangxi Normal University from July 1999 to October 2001 and a visiting scholar at the same college and university from September 2007 to July 2008. In December 2008, she was promoted to professor. Since August 23, 2012, she has served successively as a professor at the College of Physical Education and College of Electronics and Information Engineering of Beibu Gulf University (formerly Qinzhou University). Her research interests are artificial intelligence and physical education, training, and rehabilitation care. (zix@bbgu.edu.cn)

Jiang Hao received his B.S. degree in materials science from Tsinghua University, Beijing, China, in 1994, and his Ph.D. degree in electrical engineering from the University of California, San Diego, CA, USA, in 2000. He was with Broadcom Corporation, Jazz Semiconductor, Newport Beach, CA, and Conexant Systems Inc. He has been with San Francisco State University (SFSU), San Francisco, CA, since August 2007. He is currently a professor of electrical and computer engineering. His research interests include the development of low-power, high-speed, energy-efficient, and small-form-factor integrated circuit systems for biomedical and bio-inspired computing systems. (jianghao@sfsu.edu)

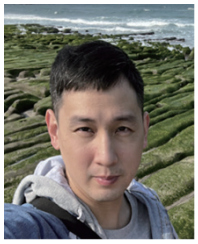

Cheng-Lun Tsai received his M.S. degree from Tamkang University, Tamsui, Taiwan, in 2017. Since 2017 to present, he has worked as a power electrical engineer at ASUS Computer. His research area is power supply design. (saka38.allen@gmail.com)